Mathematical Theory and Modeling
ISSN 2224-5804 (Paper) ISSN 2225-0522 (Online)
Vol.7, No.9, 2017

Influence of Magnetic Field on Peristaltic Transport for Eyring-Powell Fluid in A Symmetric Channel During A Porous Medium

Hayat Ali[1*] Ahmed Abdulhadi[2]

1. College of Science, Baghdad University, Baghdad 10001, Iraq
2. College of Science, Baghdad University, Baghdad 10001, Iraq

[*]E- mail of the corresponding author: hayattadel17@yahoo.com

Abstract

In this work, the influence of transverse magnetic field on peristaltic transport of an incompressible Eyring–Powell model fluid through porous medium in a symmetric channel is investigated. No slip condition and wall properties have been taken into consideration. The fundamental governing equations; mass conservation and momentum are modelled with respect to wave frame and then simplified with help of assumption long wavelength approximation and low Renold's number. The final resulting non-linear system has been solved for stream function by adopting the regular perturbation technique. The impact of physical significance of various parameters on the stream function, velocity profile, pressure gradient, and wall shear stress is utilized in details via graphs.

Keywords: Peristaltic transport, Eyring- Powell fluid, Porous medium, Magnetic field, symmetric channel

1. Introduction

The non-Newtonian fluid flow investigation regarded much interesting due to its extensive application in various field such as physiology, engineering and industry (Devakar *et al.* 2016). Certainly various constitutive relations are suggested for the flow description of such fluids diverse characteristics (Bhatti & Abbas 2016; Ismail *et al.* 2013). Powell and Eyring pointed out a fluid model known as "Eyring- Powell" fluid that gives many benefits than the other non-Newtonian fluids (Powell & Eyring 1944). This model although it is mathematically complex but it still has a certain advantages beyond the other models. It's constitutive equation deduced from the kinetic theory of fluids not by using empirical relations also it can be truly reduces into Newtonian fluid for both low and high shear rates (Adesanya *et al.* 2015). Recently numerous researchers are even now engaged for the flow analysis of non-Newtonian fluids and the peristalsis transportation. In connection with "peristalsis", the process in which the fluid is transported by means of periodic progressive wave advancing axially across the length of distensible tube (Shapiro 1969). This phenomenon has a wide application in physiological fluid transport in biological system such as urine transport from kidney to the bladder, lymph transportation in the lymphatic vessels, movement of ovum in fallopian tube and more others also it is recognized in designing many devices like dialysis machine, heart lung machine, blood pump machine, and cell separators (Parkes & Burns 1967). It is important to observe that the fluid involved in the aforementioned applications is non-Newtonian. So, numerous practical application and studies have brought about considerable interest in connection between peristaltic flow and Eyring- Powell fluid. Alsaedi *et al*. (2014) used Eyring-Powell fluid to discuss the effects of convective conditions and chemical reactions on peristaltic flow. Abbasi *et al*. (2014) constructs a mathematical model for the peristaltic transport of Eyring-Powell fluid in a curved channel. Asghar *et al*. (2013) studied the radiative effect in three-dimensional flow of MHD Eyring-Powell fluid. Hina (2016) present the combined effects of slip and magneto hydrodynamics on the peristaltic motion of Eyring-Powell fluid with heat transfer. The flow through porous medium is of pivotal importance in geomechanics, biomechanics and industry Elshehawey *et al*. (2006). The application of such flows is basically seen in filtration of fluids, seepage of water in river beds, movement of underground water and oils, physiological fluid flow in bile duct and flow of blood through small blood vessels Khan *et al*. (2013). On the other hand a great attention is given to scrutinize the peristaltic flow in presence of magneto hydrodynamic due to its significant role in construction of biomedical equipment like cancer tumor treatment, gastric medications and magnetic resonance imaging (MRI) for brain diagnosis, industrial manufacturing, geophysics (earth quick), engineering and magnetic drug targeting. In recent year, some examination focused on the effect of magnetic field on the peristaltic flow through porous medium. Bhatti *et al*. (2016) analyze a simultaneous effect of slip and MHD on peristaltic blood flow of Jeffrey fluid model through a porous medium. Ahmad *et al*. (2016) addressed

the problem of hydromagnetic peristaltic flow of variable viscosity fluid with heat transfer and porous medium. Oyelami & Dada (2016) studied the effect of MHD flow of Eyring-Powell fluid in porous medium. Adesanya *et al*. (2015) depicted the flow of MHD Eyring-Powell under couple stress through a porous medium.

The aim of this paper is to study the peristaltic transport of Eyring-Powell under the effect of magnetic field in asymmetric horizontal channel through porous medium with the consideration of no-slip condition and wall properties. The relevant equations have been constructed by employing the wave frame and then reduced by assumptions of long wave length and low Renold's number approximation. The closed form of the velocity, stream function, and pressure gradient solutions are obtained analytically with help of the relationship between them. Finally the influences of the physical parameters are discussed in detail via graphs.

2. Problem Formulation

Consider the peristaltic transport of an incompressible Eyring- Powell fluid in a two dimensional a symmetric horizontal channel with width $2d$ through a porous medium. The fluid is electrically conducting in the presence of an applied magnetic field β_0 in transverse direction to the flow. Magnetic Renold number is taken small and thus the induced magnetic field neglected. The Cartesian coordinates considered in such a manner that wave propagate parallel to $\bar{X}$ direction and the $\bar{Y}$ –axis is perpendicular to it. The waves are taken a sinusoidal with wavelength λ . The travelling waves with constant speed c along the wall of the channel. The walls of channel are flexible subject to viscous damping effect.

The mathematical form of wall surface is given by

$$\bar{Y} = \pm\bar{H}(\bar{X},\bar{t}) = \pm\left(d + a\sin\frac{2\pi}{\lambda}\left(\bar{X} - c\bar{t}\right)\right) \tag{1}$$

Where a represents the wave amplitude, d is the mean half width, (c) the velocity of the peristaltic wave, $(\bar{t})$ is the time and $\pm\bar{H}(\bar{X},\bar{t})$ is the displacements of the upper and lower walls respectively.

The governing equation of the motion for incompressible Eyring- Powell fluid model in laboratory frame $(\bar{X},\bar{Y},\bar{t})$ through porous medium in the presence of applied normal magnetic field can be summarized as

$$\frac{\partial\bar{U}}{\partial\bar{X}} + \frac{\partial\bar{V}}{\partial\bar{Y}} = 0 \tag{2}$$

$$\rho\left(\frac{\partial\bar{U}}{\partial\bar{t}} + \bar{U}\frac{\partial\bar{U}}{\partial\bar{X}} + \bar{V}\frac{\partial\bar{U}}{\partial\bar{Y}}\right) = -\frac{\partial\bar{P}}{\partial\bar{X}} + \frac{\partial\bar{S}_{\bar{X}\bar{X}}}{\partial\bar{X}} + \frac{\partial\bar{S}_{\bar{X}\bar{Y}}}{\partial\bar{Y}} - \sigma\beta_0^2\bar{U} - \frac{\mu}{\kappa_0}\bar{U} \tag{3}$$

$$\rho\left(\frac{\partial\bar{V}}{\partial\bar{t}} + \bar{U}\frac{\partial\bar{V}}{\partial\bar{X}} + \bar{V}\frac{\partial\bar{V}}{\partial\bar{Y}}\right) = -\frac{\partial\bar{P}}{\partial\bar{Y}} + \frac{\partial\bar{S}_{\bar{Y}\bar{X}}}{\partial\bar{X}} + \frac{\partial\bar{S}_{\bar{Y}\bar{Y}}}{\partial\bar{Y}} - \frac{\mu}{\kappa_0}\bar{V} \tag{4}$$

Where (ρ) signify the density of the fluid, (μ), (σ), $(\bar{P})$, $(\bar{U})$, $(\bar{V})$, (κ_0) , (β_0) ,denote the dynamic viscosity, electric conductivity, pressure, axial velocity, transvers velocity, permeability of porous medium, and the magnitude of magnetic field respectively.

The stress tensor for Eyring- Powell fluid is described by (Hina 2016) as follows:

$$\bar{S}_{ij} = \mu\frac{\partial\bar{u}_{ij}}{\partial\bar{x}_j} + \frac{1}{\beta}\sinh^{-1}\left(\frac{1}{c_1}\frac{\partial\bar{u}_i}{\partial\bar{x}_j}\right) \qquad for \quad i,j = 1,2 \tag{5}$$

where $\bar{u}_1 = \bar{U}$, $\bar{u}_2 = \bar{V}$, $\bar{x}_1 = \bar{X}$, $\bar{x}_2 = \bar{Y}$

$(\bar{S}_{ij})$ designates the extra stress tensor. Also, (c_1) and (β) represent the material parameters of Eyring-Powell fluid and (μ) is the dynamic viscosity. The term $(\sinh^{-1})$ is approximated using the second order approximation of the hyperbolic sine function as bellows:

$$\sinh^{-1}\left(\frac{1}{c_1}\frac{\partial \bar{u}_i}{\partial \bar{x}_j}\right) \cong \frac{1}{c_1}\frac{\partial \bar{u}_i}{\partial \bar{x}_j} - \frac{1}{6}\left(\frac{1}{c_1}\frac{\partial \bar{u}_i}{\partial \bar{x}_j}\right)^3 \quad \left|\frac{1}{c_1}\frac{\partial \bar{u}_i}{\partial \bar{x}_j}\right| << 1 \tag{6}$$

Then Equation. (5) will be rewritten as

$$\bar{S}_{ij} = \mu\frac{\partial \bar{u}_i}{\partial \bar{x}_j} + \frac{1}{\beta c_1}\frac{\partial \bar{u}_i}{\partial \bar{x}_j} - \frac{1}{6\beta {c_1}^3}\left(\frac{\partial \bar{u}_i}{\partial \bar{x}_j}\right)^3 \tag{7}$$

So, the stress components of Equation. (7) take the following forms

$$\bar{S}_{\bar{X}\bar{X}} = \mu\frac{\partial \bar{U}}{\partial \bar{X}} + \frac{1}{\beta c_1}\frac{\partial \bar{U}}{\partial \bar{X}} - \frac{1}{6\beta {c_1}^3}\left(\frac{\partial \bar{U}}{\partial \bar{X}}\right)^3 \tag{8}$$

$$\bar{S}_{\bar{X}\bar{Y}} = \mu\frac{\partial \bar{U}}{\partial \bar{Y}} + \frac{1}{\beta c_1}\frac{\partial \bar{U}}{\partial \bar{Y}} - \frac{1}{6\beta {c_1}^3}\left(\frac{\partial \bar{U}}{\partial \bar{Y}}\right)^3 \tag{9}$$

$$\bar{S}_{\bar{Y}\bar{X}} = \mu\frac{\partial \bar{V}}{\partial \bar{X}} + \frac{1}{\beta c_1}\frac{\partial \bar{V}}{\partial \bar{X}} - \frac{1}{6\beta {c_1}^3}\left(\frac{\partial \bar{V}}{\partial \bar{X}}\right)^3 \tag{10}$$

$$\bar{S}_{\bar{Y}\bar{Y}} = \mu\frac{\partial \bar{V}}{\partial \bar{Y}} + \frac{1}{\beta c_1}\frac{\partial \bar{V}}{\partial \bar{Y}} - \frac{1}{6\beta {c_1}^3}\left(\frac{\partial \bar{V}}{\partial \bar{Y}}\right)^3 \tag{11}$$

The associated boundary conditions comprising wall no-slip and its flexibility conditions are described in the forms

$$\bar{U} = 0, \bar{V} = H_{\bar{t}} \quad \text{at} \quad \bar{Y} = \pm\bar{H}(\bar{X},\bar{t}) \tag{12}$$

$$\left[-\tau\frac{\partial^3}{\partial \bar{X}^3} + m_1\frac{\partial^3}{\partial \bar{X}\partial \bar{t}^2} + d'\frac{\partial^2}{\partial \bar{X}\partial \bar{t}}\right]\bar{H}(\bar{X},\bar{t}) = -\rho\frac{\partial \bar{U}}{\partial \bar{t}} + \frac{\partial \bar{S}_{\bar{X}\bar{X}}}{\partial \bar{X}} + \frac{\partial \bar{S}_{\bar{X}\bar{Y}}}{\partial \bar{Y}} \tag{13}$$

where (τ) is the elastic tension, m_1 the mass per unit area and (d') is the coefficient of viscous damping. The flow is time dependent with respect to laboratory coordinate $(\bar{x},\bar{y},\bar{t})$, whereas in the wave frame of coordinate $(\bar{x},\bar{y})$ moving with the wave velocity the flow considered steady. Taking $(\bar{u},\bar{v})$ as the velocity components and $\bar{P}(\bar{x},\bar{y})$ the pressure in the wave frame, to write the governing equation in wave frame we need the following transformation relationship between the laboratory and wave coordinates

$$\bar{x} = \bar{X} - c\bar{t}, \bar{y} = \bar{Y}, \bar{u} = \bar{U} - c, \bar{v} = \bar{V}, \bar{p}(\bar{x},\bar{y}) = \bar{P}(\bar{X},\bar{Y},\bar{t}) \tag{14}$$

So, the equations of the motion in the wave frame will be formed as below

$$\frac{\partial \bar{u}}{\partial \bar{x}}+\frac{\partial \bar{v}}{\partial \bar{y}}=0 \tag{15}$$

$$\rho\left((\bar{u}+c)\frac{\partial \bar{u}}{\partial \bar{x}}+\bar{v}\frac{\partial \bar{u}}{\partial \bar{y}}\right)=-\frac{\partial \bar{P}}{\partial \bar{x}}+\frac{\partial \bar{S}_{\bar{x}\bar{x}}}{\partial \bar{x}}+\frac{\partial \bar{S}_{\bar{x}\bar{y}}}{\partial \bar{y}}-\sigma\beta_0^2(\bar{u}+c)-\frac{\mu}{\kappa_0}(\bar{u}+c) \tag{16}$$

$$\rho\left((\bar{u}+c)\frac{\partial \bar{v}}{\partial \bar{x}}+\bar{v}\frac{\partial \bar{v}}{\partial \bar{y}}\right)=-\frac{\partial \bar{P}}{\partial \bar{y}}+\frac{\partial \bar{S}_{\bar{y}\bar{x}}}{\partial \bar{x}}+\frac{\partial \bar{S}_{\bar{y}\bar{y}}}{\partial \bar{y}}-\frac{\mu}{\kappa_0}\bar{v} \tag{17}$$

The geometric of the walls in wave frame will be transformed as

$$\bar{y}=\pm\bar{h}(\bar{x})=\pm\left(d+a\sin\frac{2\pi}{\lambda}(\bar{x})\right) \tag{18}$$

Finally the boundary conditions will be transformed as below

$$\left.\begin{array}{c}\bar{u}=0\,,\ \bar{v}=0\\ -\tau\dfrac{\partial^3 h(\bar{x})}{\partial \bar{x}^3}=\dfrac{\partial \bar{S}_{\bar{x}\bar{y}}}{\partial \bar{y}}+\dfrac{\partial \bar{S}_{\bar{x}\bar{x}}}{\partial \bar{x}}\end{array}\right\} \quad \text{at} \quad \bar{y}=\pm\bar{h}(\bar{x}) \tag{19}$$

Introducing the stream function $\psi(\bar{x},\bar{y},\bar{t})$ in the laboratory coordinates and defining the dimensionless quantities as below:

$$x=\frac{\bar{x}}{\lambda},y=\frac{\bar{y}}{d},u=\frac{\bar{u}}{c},v=\frac{\bar{v}}{c},h=\frac{\bar{h}}{d},p=\frac{d^2\bar{p}}{\lambda\mu c},\delta=\frac{d}{\lambda},,S_{ij}=\frac{d\bar{S}_{ij}}{\mu c},\mathrm{Re}=\frac{\rho c d}{\mu},W=\frac{1}{\mu\beta c_1},A=\frac{W}{6}\left(\frac{c}{c_1 d}\right)^2,E_1=\frac{-\pi d^3}{\lambda^3\mu c},$$

$$M=\frac{\beta_0{}^2 d^2\sigma}{\mu},\phi=\frac{a}{d},\ m^2=(\frac{1}{\kappa}+M),\kappa=\frac{\kappa_0}{d^2}$$

(20)

In which $(A\ and\ W)$ are the dimensionless Eyring- Powell fluid parameters, (x) the non-dimensional axial coordinate, (y) the non-dimensional transverse coordinate, (u,v) are the non-dimensional velocity components, (P) non-dimensional pressure, (δ) is the wave number, (Re) the Renold's number, (κ) the dimensionless permeability parameter, (M) the Hartmann number, (ϕ) the amplitude ratio, and (E_1) the tension characterizing. Employing the relationship between the stream function and the velocity component as follows

$$u=\frac{\partial \psi}{\partial y}\quad and\quad v=-\delta\frac{\partial \psi}{\partial x} \tag{21}$$

Making use of the above mentioned non- dimensional parameters, the continuity equation is obviously satisfied, and motion Equations (16) to (17) will be reduced as follows

$$\delta\frac{\partial u}{\partial x}+\frac{\partial v}{\partial y}=0 \tag{22}$$

$$\delta \operatorname{Re}\left((\psi_y+1)\psi_{xy}-\psi_x\psi_{yy}\right)=-P_x+\delta\frac{\partial S_{xx}}{\partial x}+\frac{\partial S_{xy}}{\partial y}-m^2\left(\psi_y+1\right) \tag{23}$$

$$\delta^3 \operatorname{Re}\left(-(\psi_y+1)\psi_{xx}+\psi_x\psi_{xy}\right)=-P_y+\delta^2\frac{\partial S_{yx}}{\partial x}+\delta\frac{\partial S_{yy}}{\partial y}+\frac{\delta^2}{\kappa}\psi_x \tag{24}$$

The non-dimensional stress components are

$$S_{xx}=\delta(1+W)\psi_{xy}-\delta^3\,A{\psi_{xy}}^3 \tag{25}$$

$$S_{xy}=(1+W)\psi_{yy}-A\,{\psi_{yy}}^3 \tag{26}$$

$$S_{yx}=-\delta(1+W)\psi_{xy}-\delta^3\,A{\psi_{xy}}^3 \tag{27}$$

Finally the dimensionless of corresponding boundary conditions with respect to wave frame are

$$\psi_y=0 \quad and \quad \psi_x=0 \qquad \text{at} \qquad y=\pm h(x)=\pm\left(1+\phi\sin 2\pi x\right) \tag{28}$$

$$E_1\frac{\partial^3 h(x)}{\partial x^3}=\frac{\partial S_{xy}}{\partial y} \tag{29}$$

Where $h(x)$ is the dimensionless of wall geometry. Under long wavelength and low Renold's number approximation Equations (23) & (24) with the associated boundary conditions will be reduced into the following equations.

$$P_x=\frac{\partial S_{xy}}{\partial y}-m^2(\psi_y+1)=0 \tag{30}$$

$$P_y=0 \tag{31}$$

with boundary conditions

$$\left.\begin{aligned}\psi_y&=0\\ E_1\frac{\partial^3 h(x)}{\partial x^3}&=\frac{\partial S_{xy}}{\partial y}\end{aligned}\right\} \quad \text{at} \quad y=\pm h(x)=\pm\left(1+\phi\sin 2\pi x\right) \tag{32}$$

By combining Equations (30) & (31) ,and making use of Equation (26) we get

$$(1+W)\psi_{yyyy}-A\frac{\partial^2}{\partial y^2}(\psi_{yy})^3-m^2\psi_{yy}=0 \tag{33}$$

3. Solution Technique

Employing the perturbation method for small Eyring- Powell fluid parameter the solution of non-dimensional governing equation will be found, we expand the stream function in the form

$$\psi=\psi_0+A\,\psi_1+O(A^2) \tag{34}$$

Substituting Equation (34) into Equations (32) & (33) , we have the following two resulting system

3.1 Zeroth Order System and Solution

The resulting zeroth order system has the form

$$(1+W)\psi_{0yyyy}-m^2\psi_{0yy}=0 \tag{35}$$

Associated with the boundary conditions

$$\left.\begin{array}{c}\psi_{0y}=0\\ E_1\dfrac{\partial^3 h(x)}{\partial x^3}=(1+W)\psi_{0yyy}\end{array}\right\} \quad \text{at} \quad y=\pm h(x) \tag{36}$$

Solving the above system, the solution will take the form

$$\psi_0=\frac{(1+W)}{m^2}\left(e^{\frac{m}{\sqrt{1+W}}y}c_1+e^{\frac{-m}{\sqrt{1+W}}y}c_2\right)+c_3+c_4y \tag{37}$$

3.2 First Order System and Solution

The first order system takes the form

$$(1+W)\psi_{1yyyy}-m^2\psi_{1yy}-\frac{\partial^2(\psi_{0yy})^2}{\partial y^2}=0 \tag{38}$$

With the boundary conditions

$$\left.\begin{array}{c}\psi_{1y}=0\\ (1+W)\psi_{1yyy}-\dfrac{\partial}{\partial y}\left(\psi_{0yy}\right)^3=0\end{array}\right\} \quad \text{at} \quad y=\pm h(x) \tag{39}$$

The first order solution obtained from the above system is

$$\psi_1=\frac{e^{-3\upsilon y}(c_2{}^3\upsilon^2+c_1{}^3e^{6\upsilon y}\upsilon^2+6c_1{}^2c_2e^{4\upsilon y}\upsilon^2(-5+2\upsilon y)-6c_1c_2{}^2e^{2\upsilon y}\upsilon^2(5+2\upsilon y)+8e^{2\upsilon y}m^2(e^{2\upsilon y}b_1+b_2))}{8m^2\upsilon^2}+b_3+b_4y \tag{40}$$

where, $(\upsilon^2=\frac{m^2}{(1+W)})$ and the values of $(c_1,c_2,c_3,c_4,b_1,b_2,b_3,b_4)$ are non-constant and their values can be calculated algebraically using Mathematica.

4. Result and Discussion

This section prepared to describe the computational results of our problem graphically using MATHEMATICA program. It is consist of four parts. The first one illustrates the impact of some interesting physical parameters on the axial velocity distribution. However in the second parts the evolution of wall shear stress at the wall $h(x)$ with different flow parameters discussed. The effect of physical parameters on pressure gradient analyzes in the third part. Finally the trapping of the flow under the impact of various parameters is scripted.

4.1 Velocity Profile

Figures.1 to 6, manifest the influence of wall membrane parameter E_1, Eyring- Powell parameters A, W the amplitude ratio (ϕ), magnetic field parameter M and permeability parameter κ on velocity profile $u(y)$ that plotted for fixed value of $x = 0.02$. The graphical descriptions show that the velocity profile is parabolic in

nature. Figure.1 gives an idea that the velocity is directed properly with wall elestance coefficient E_1 , and the maximum impact can be seen when $y = 0.6$ in another word the velocity increases as (E_1) increases since the walls of the channel are compliant and exhibit elastic effect that reduce the resistance to flow and hence speed up the velocity. Figures. 2 & 6, portray the completely opposite impact on velocity profile with changing in fluid parameters (A), and (W) The figures captured that the velocity increases as A increases (since increases in A enhances the kinetic energy of particles and hence increases the velocity), whereas increases in (W) reduces the axial velocity. The effect of magnetic field parameter (M) on velocity profile depicted in Figure.3 one can observe that an increases in (M) reduces the velocity distribution because the Lorentz force increases and as a result the resistance to the flow become larger. It is also noticed from Figure.4, that the velocity profile increases as the porosity parameter (κ) increases. From Figure.5, we notice that larger magnitude of amplitude ratio speed up the velocity of the fluid and the maximum value appears at $y = 0.6$.

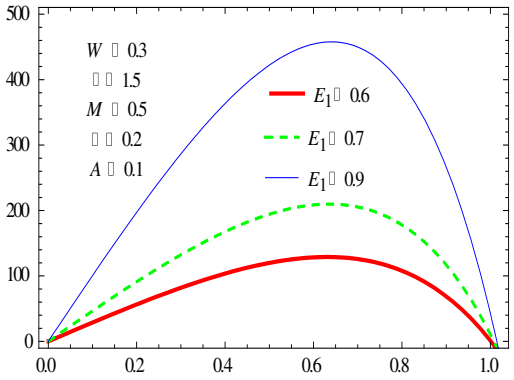

Figure.1 Velocity Profile $u(y)$ for Variation (E_1)

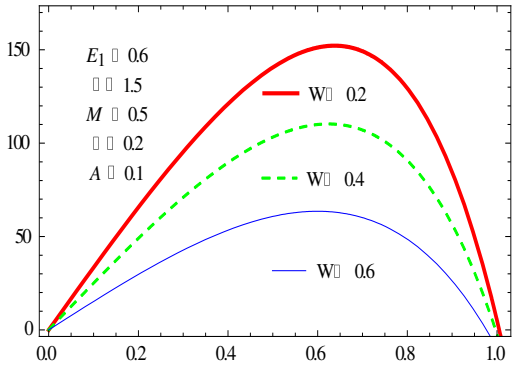

Figure.2 Velocity Profile $u(y)$ for Variation (W)

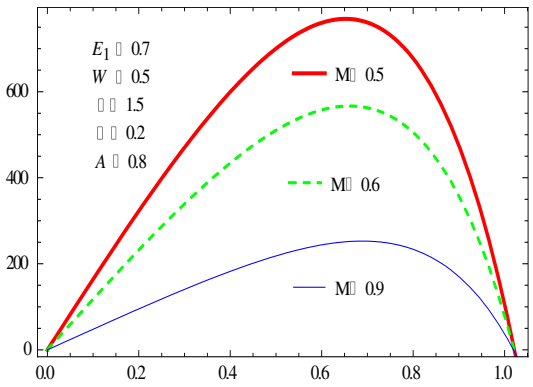

Figure.3 Velocity Profile $u(y)$ for Variation (M)

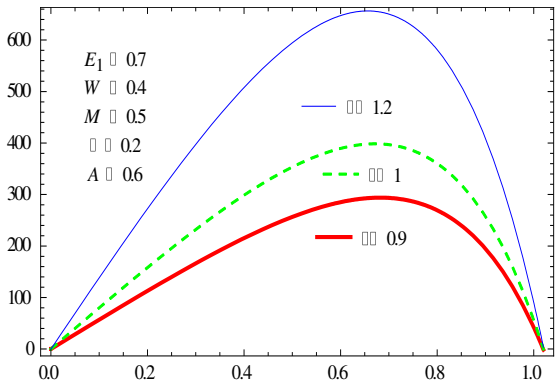

Figure.4 Velocity Profile $u(y)$ for Variation (κ)

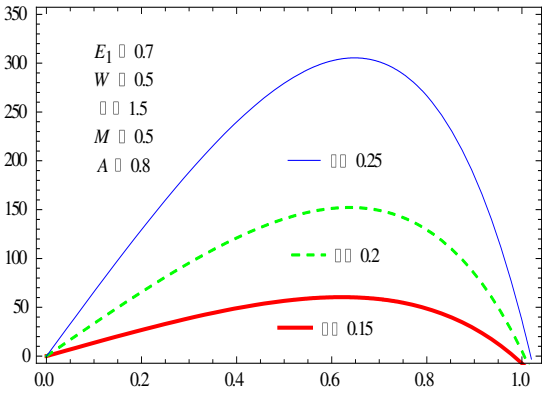

Figure.5 Velocity Profile $u(y)$ for Variation (ϕ)

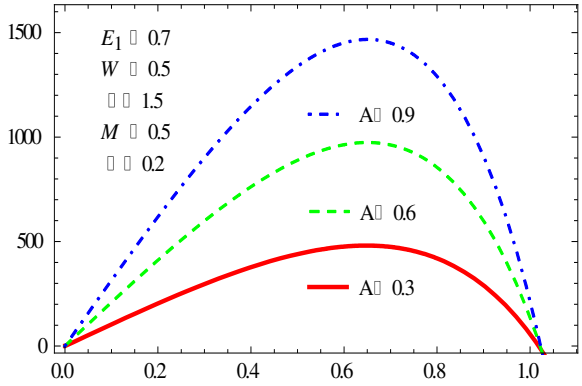

Figure.6 Velocity Profile $u(y)$ for Variation A

4.2 Pressure Gradient

Physical impact of pertinent parameters on the pressure gradient in wave frame inspected through Figures. 7 to 12. The figures show an oscillatory function. From Figures.7 & 11, one can deduced that if the wall elastence parameter E_1, and the

permeability parameter κ increase an important consideration can be made which is in the vicinity of the channel walls for $(0 \le x \le 0.1) \cup (0.85 \le x \le 1)$ more pressure needed for the fluid to flow while in the central part of the channel for $(0.4 \le x \le 0.6)$ due to low pressure difference, the fluid flows so easy. Also at $(0.15 \le x \le 0.35)\ and\ (0.65 \le x \le 0.85)$ the pressure is diminishing. Figure.8, shows that when the magnitude of magnetic field parameter (M) increases the pressure gradient decreases especially at the walls of the channel but this action reverse in the central part of the channel where $\frac{dP}{dx}$ increases. Figures.9 & 10, seek a totally opposite influence for Eyring- Powell parameters (W) & A to each other's on the pressure gradient, they show increasing of $\frac{dP}{dx}$ as A increases and (W) decreases near the channel walls, however in the central part the opposite results noticed (i.e. the magnitude of $\frac{dP}{dx}$ increaces with inceases of (W) and decreases of A). Figure.12, demonstrates the physical reaction of amplitude ratio on the magnitude of pressure gradient. An increasing in $\frac{dP}{dx}$ is noticed upon increasing of (ϕ) value at the walls while it reduces in the central part of the channel.

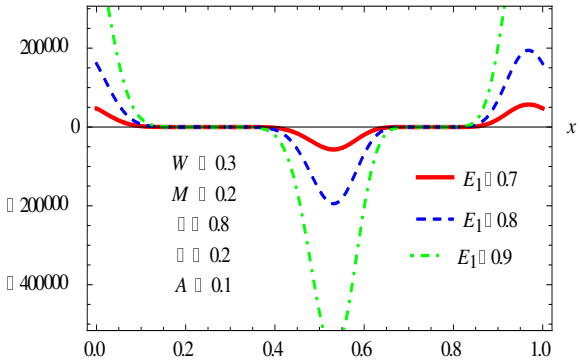

Figure.7 Pressure Gradient $\frac{dP}{dx}$ upon E_1

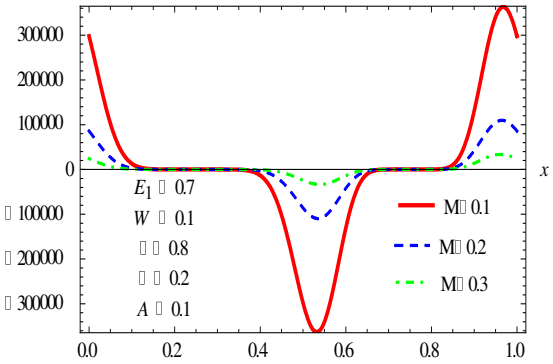

Figure.8 Pressure Gradient $\frac{dP}{dx}$ upon (M)

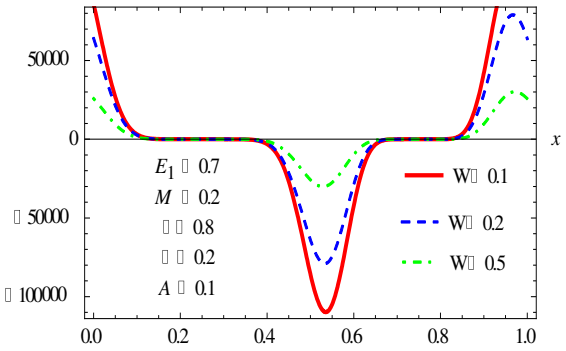

Figure.9 Pressure Gradient $\frac{dP}{dx}$ upon (W)

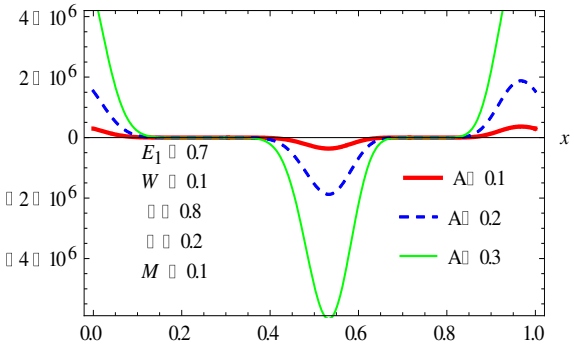

Figure.10 Pressure Gradient $\frac{dP}{dx}$ upon A

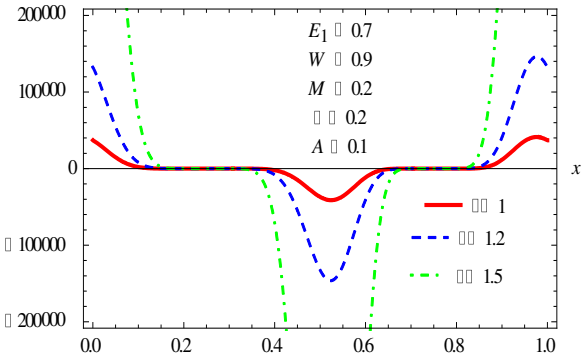

Figure.11 Pressure Gradient $\frac{dP}{dx}$ upon (κ)

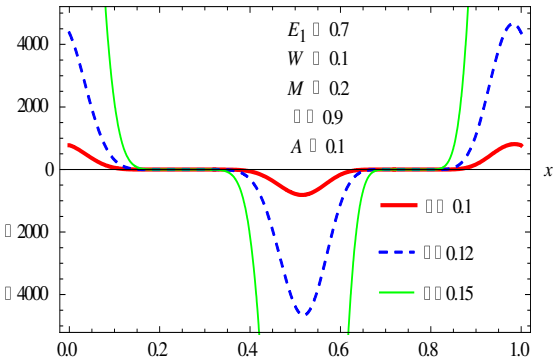

Figure.12 Pressure Gradient $\frac{dP}{dx}$ upon (ϕ)

4.3 Wall Shear Stress

Figures.13 to 18, recorded the impact of different emerging parameters involved in shear stress equation upon the horizontal coordinate x- axis. The values of shear stress evaluated at a fixed value for $y = 0.02$. Figure.13, detected that the local wall shear stress attains maximum value in the central part of the channel , and then it begin to retard toward the walls of the channel another observation can be made from the figure is that S_{xy} increasing as the elastance parameter of the wall E_1 increasing at the central part however the situation is reverse near the walls of the channel (i.e. the shear stress decreasing. For large value of magnetic parameter (M)) the shear stress quantity reduces this effect illustrated through Figure.14.However Figuress.15 & 16, suggest two opposite behavior of S_{xy} for W, A, in which for ascending value of W the shear stress quantity increases in the central part of channel for $x = 0.5$ and decreases for A, while S_{xy} exhibits an opposite response near the walls for $(W, and\ A)$. While Figures.17 & 18, depict an increasing behavior for S_{xy} via increase of amplitude ratio (ϕ) and permeability parameter κ at the center and reduction function near the walls.

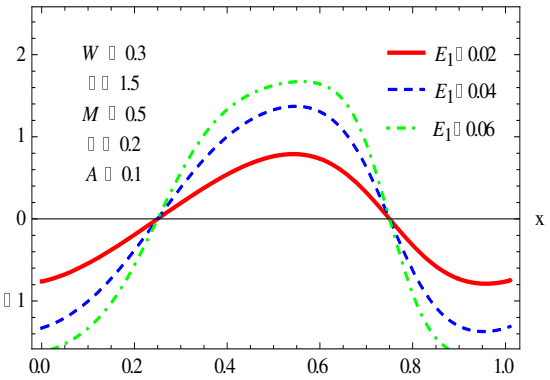

Figure.13 Shear Stress upon E_1

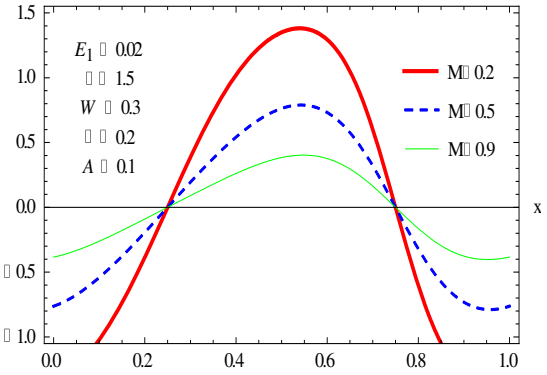

Figure.14 Shear Stress upon (M)

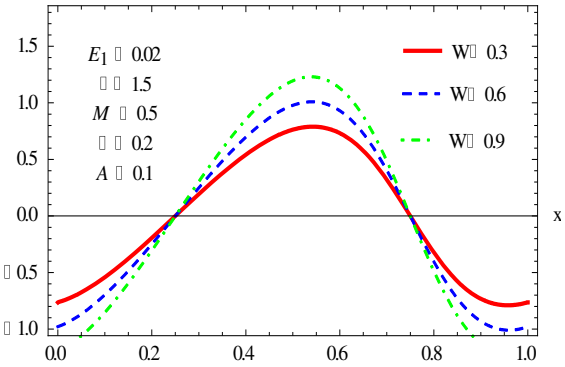

Figure.15 Shear Stress upon (W)

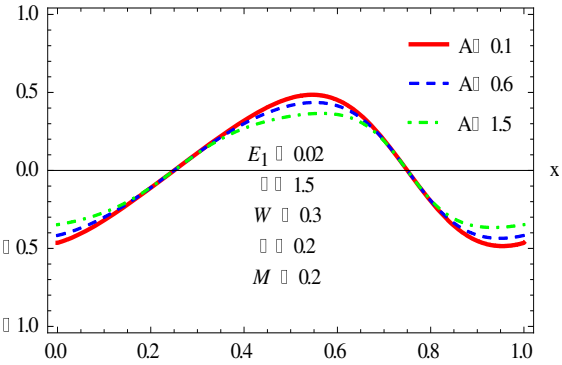

Figure.16 Shear Stress upon A

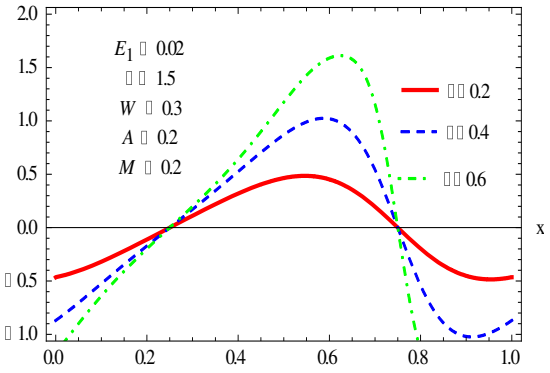

Figure.15 Shear Stress upon (ϕ)

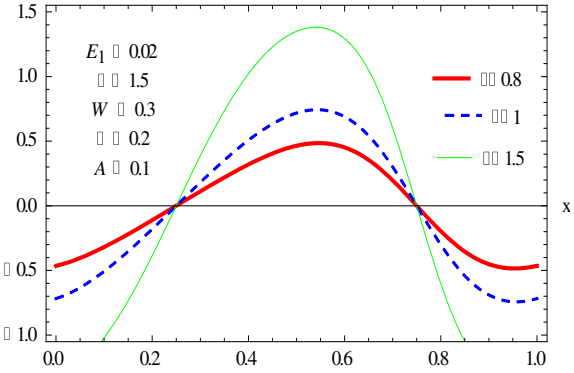

Figure.16 Shear Stress upon (κ)

4.4 Trapping

A phenomenon of trapped bolus is a formation of closed and circular splitting of streamlines which moves along the peristaltic wave. Figures.17 to 22, display the generation of trapped bolus with variation of physical parameters involved in the stream function ψ in the wave frame. Figure.17 illustrates that the size of the bolus increasing with an increasing of wall parameter E_1. Moreover, Figure.18, shows that the trapped bolus size reduces upon increasing the magnetic parameter (M). In Figurs.19 & 20, we found that there is a hardly small impact considered for fluid parameters $(W, and\ A)$ on streamlines. While Figures.21 & 22, depict that the bolus size increases as the magnitude of (ϕ, κ) increase.

(a) (b) (c)

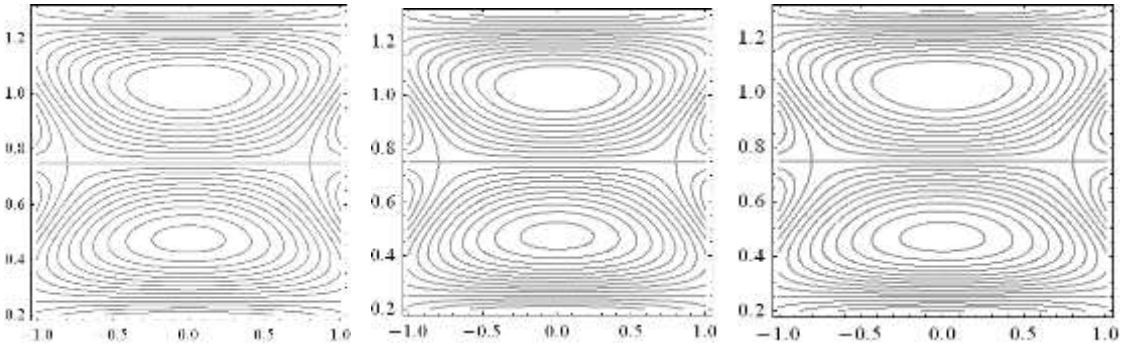

Figure.16 Streamlines for Variation of E_1 and Fixed $\{W = 0.3, A = 0.1, \phi = 0.2, M = 0.5, \kappa = 1.5\}$

(a) $E_1 = 0.02$ (b) $E_1 = 0.04$ (c) $E_1 = 0.06$

(d) (e) (f)

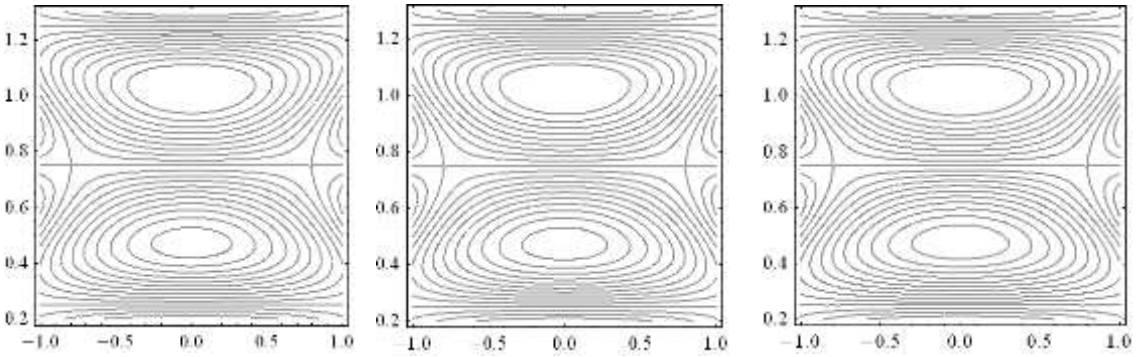

Figure.17 Streamlines for Variation of M and Fixed $\{W = 0.3, A = 0.1, \phi = 0.2, E_1 = 0.02, \kappa = 0.8\}$

(d) $M = 0.2$ (e) $M = 0.4$ (f) $M = 0.6$

(g) (h) (i)

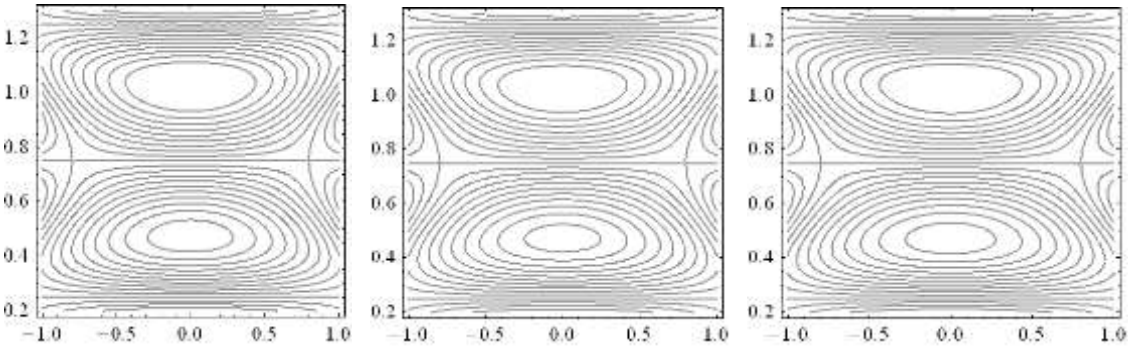

Figure.18 Streamlines for Variation of A and Fixed $\{W = 0.3, M = 0.5, \phi = 0.2, E_1 = 0.02, \kappa = 0.8\}$

(g) $A = 0.2$ (h) $A = 0.4$ (i) $A = 0.6$

(J) (k) (l)

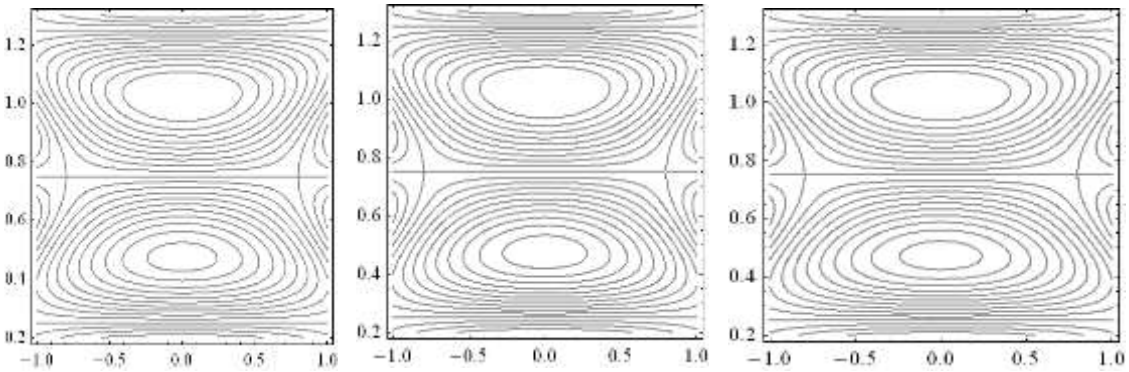

Figure.19 Streamlines for Variation of W and Fixed $\{A = 0.1, M = 0.1, \phi = 0.2, E_1 = 0.02, \kappa = 0.8\}$ (J) $W = 0.3$ (k) $W = 0.6$ (l) $W = 0.9$

(m) (n) (o)

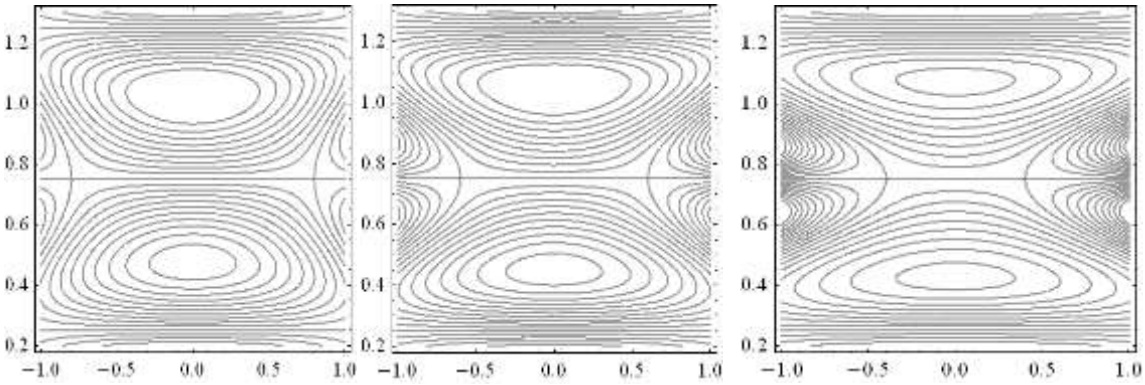

Figure.20 Streamlines for Variation of ϕ and Fixed $\{A = 0.1, M = 0.5, W = 0.3, E_1 = 0.02, \kappa = 0.8\}$

(m) $\phi = 0.2$ (n) $\phi = 0.4$ (o) $\phi = 0.6$

(p) (q) (s)

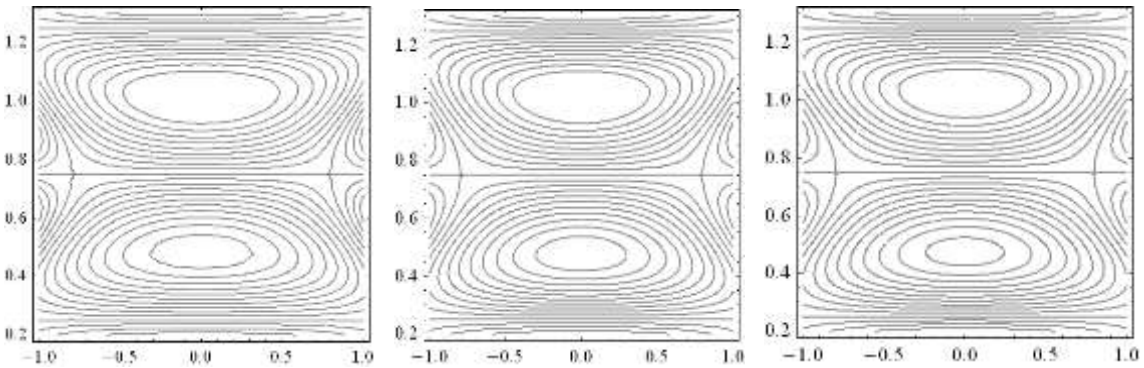

Figure.21 Streamlines for Variation of κ and Fixed $\{A = 0.1, M = 0.5, W = 0.3, E_1 = 0.02, \phi = 0.2\}$

(p) $\kappa = 0.5$ (q) $\kappa = 1$ (s) $\kappa = 1.5$

5. Conclusion

The impacts of magnetic field on the peristaltic flow for Eyring- Powell fluid through porous medium in a horizontal symmetric channel associated with no slip condition and wall properties are investigated. The fundamental governing equation flow problem has been constructed and simplified under the assumptions of

long wavelength and low Renolds number. The results are discussed graphically taking into consideration the effects of variation of some interesting flow parameters. Major conclusion observations have been listed below:

1. The longitudinal velocity enhances at the center part of the channel with the increase in A, κ, E_1, and (ϕ) whereas it decreases near the channel walls. It is observed that (M), and (W) have opposite influences when compared with the above parameters.
2. The magnitude of pressure gradient increases near the walls of channel as A, κ, E_1 and (ϕ) increases whereas it reduces in the central part of the channel. The response is completely reverse with increasing of (W), and (M) magnitudes.
3. The value of axial shear stress increases in the center part of the channel, however it reduces towards the channel walls. it is noted that shear stress increases for E_1, W, κ, and (ϕ) while it decreases with (A) and (M).
4. The size of the trapped bolus increases for increases of E_1, κ and (ϕ). However opposite effect is noticed for magnetic field parameter (M). Hardly change has been seen on the trapped bolus for both fluid parameters (A) and (W).

Suggested future works include study the effect of heat transfer on peristaltic transport for MHD Eyring- Powell fluid through a porous medium in an inclined channel with convective conditions.

References

Alsaedi, A. ,Tanveer, A., Hayat, T., & Yasmin, H.,.(2014), " Effects of Convective Conditions and Chemical Reaction on Peristaltic flow of Eyring- Powell fluid", Journal of Applied Bionics and Biomechanics, 11, 221-233.

Abbasi, F., Alsaedi, A., & Hayat, T., (2014), " Peristaltic Transport of Eyring- Powell fluid in a curved channel", Journal of Aerospace Engineering, 27, 893-1321.

Adesanya, S., Falade, A., & Rach, R., (2015), " Effect of Couple Stresses on Hydromagnetic Eyring- Powell Fluid Flow Through a Porous Channel", Journal of Theoretical & Applied Mechanics, 42(2), 135-150.

Asghar, S., Awais ,M.,& Hayat ,T., (2013), " Radiative effect in a three- dimensional flow of MHD Eyring-Powell fluid", Journal of Egyptian Mathematical Society, 21, 379-384.

Ahmad, B., Hayat, T., & Abbasi, F., (2016), " Hydromagnetic Peristaltic Transport of Variable Viscosity Fluid with Heat Transfer and Porous Medium", Journal of Applied Mathematics & Information Sciences, 10(6), 2173-2181.

Bhatti, M., & Abbas, M., (2016), "Simultaneous effect of slip and MHD on peristaltic blood flow of Jeffrey fluid model through a porous medium", Journal of Alexandria Engineering, 55, 1017- 1023.

Devakar, M., Ramesh, K., Chouhan, S., & Raje, A., (2016), " Fully developed flow of non- Newtonian fluids in a straight uniform square duct through porous medium", Journal of Association of Arab Universities for Basic and Applied Sciences, 1815-3852.

Elshehawey. E., Eldabe. N., Elghazy, E., & Ebaid, A., (2006), " Peristaltic transport in a symmetric channel through a porous medium", Journal of Applied. Mathematics, and Computation, 182, 140- 150.

Hina, S., (2016), "MHD peristaltic transport of Eyring-Powell fluid with heat/mass transfer, wall properties and slip conditions", Journal of Magnetism and Magnetic Materials, 404, 148- 158.

Ismail, G., Darwesh, F., & Dabe, N., (2013), " Peristaltic Transport of a Magneto Non- Newtonian Fluid through A porous medium in horizontal finite channel", Journal of IOSR Mathematics, 8(6), 32-39.

Khan, A., Ellahi, R., & Usman, M., (2013), " The Effects of Variable Viscosity on the Peristaltic Flow of Non-Newtonian Fluid Through A Porous Medium in an Inclined Channel with Slip Boundary Conditions", Journal of Porous Media, 16 (2), 59- 67

Oyelami, F.H., & Dada, M.S., (2016), " Transient Magnetohydrodynamic Flow of Eyring- Powell Fluid in A Porous Medium", Ife Journal of Science, 18(2) .

Parkes, T., & Burns,,J., .(1967), " Peristaltic motion", J. Fluid Mechanics, 29(4), 731- 743.

Powell, R.E., Eyring, H., (1944), " Mechanisms for the relaxation theory of viscosity", Journal of Nature, 154, 427-428.

Shapiro, A., Jaffrin, M., & Weinberg, S., (1969), " Peristaltic pumping with long wavelength at low Renolds number", Journal of Fluid Mechanics, 37, 799- 825.